Laboratory and Numerical Investigation of the Hydro-mechanical Behaviour of the Cobourg Limestone

G. Su[1], S. Nguyen[1], Z. Li[1], M.H.B. Nasseri[2], R.P. Young[2]

[1]Canadian Nuclear Safety Commission, Ottawa, Canada
[2]Department of Civil Engineering, University of Toronto, Canada

The excavation of galleries and shafts of a deep geological repository (DGR) can induce damage in the surrounding rock. The excavation damage zone (EDZ) has higher permeability and reduced strength compared to the undisturbed rock and those factors must be considered in the safety assessment of the DGR. Ontario Power Generation is currently proposing a DGR for the management of its low and intermediate level nuclear wastes in a sedimentary rock formation of the Michigan Basin, known as the Cobourg limestone. The authors are conducting experimental and theoretical research in order to confirm the hydro-mechanical behaviour of the host rock, both in the undamaged and damaged state. The experimental program consisted of triaxial tests with a controlled loading rate up to and beyond failure. During the tests, the permeability and the seismic wave velocity were measured for six specimens cored parallel and perpendicular to the bedding plane. The experimental results show that the Cobourg limestone is an anisotropic material with respect to the mechanical behaviour. However, the measured permeability of the intact Cobourg limestone does not show significant difference for the six specimens. The permeability measured post failure is 2~3 orders of magnitude higher than that of the intact rock. The evolution of the compressional and shear-wave velocities and shear wave splitting as a function of the axial stress confirms the anisotropic behaviour of the Cobourg limestone. An anisotropic elasto-plastic model based on the microstructure tensor approach was developed to simulate the tests. The preliminary simulations successfully re-produced the experimental results.

1. Introduction

Argillaceous rocks are candidate host and/or cap formations for the geological disposal of nuclear wastes in many countries. The understanding of the long-term hydro-mechanical behaviour of such rocks is one of the essential requirements for the assessment of their performance as a barrier against radionuclide migration. The extent and the hydro-mechanical evolution of an excavation damage zone are important aspects to be assessed for the design of plugs and seals of the repository, if deemed necessary. In Canada, the Cobourg limestone is selected as the host rock for a deep geological repository for the management of low and intermediate level nuclear wastes proposed by Ontario Power Generation. In order to understand the hydro-mechanical behaviour of the Cobourg limestone, the Canadian Nuclear Safety Commission (CNSC) collaborated with the University of Toronto to perform experimental investigations of its hydro-mechanical behaviour with a special attention to the evolution of hydraulic property with mechanical damage induced by the excavation of the repository. Using the data from the triaxial tests, we developed constitutive relationships for the hydro-mechanical

behaviour of the Cobourg limestone and simulated the evolution of permeability with the mechanical damage of the rock.

2. Description of samples and testing equipment

The Cobourg limestone is a mottled light to dark grey, very fine- to coarse-grained, very hard, fossiliferous argillaceous limestone (NWMO 2011). The block samples for the experiment were collected at the St. Mary's quarry near the Darlington nuclear power plant. The cylindrical testing specimens were cored parallel and perpendicular to the bedding plane in the laboratory. Porosity and density of the limestone were measured according to the ISRM standard procedure (1981a) and are shown in Table 2-1.

Table 2-1 Physical properties of the Cobourg limestone measured at the RFDF

Specimen number	Length (cm)	Diameter (cm)	Porosity (%)	Dry density (g/cm^3)	Density at saturation (g/cm^3)
CLV-1-T	12.50	5.04	0.82	2.33	2.34
CLV-3-T	12.50	5.04	1.26	2.31	2.32
CLV-4-U	12.50	5.04	0.83	2.32	2.33
CLH-1-T	12.50	5.04	0.85	2.33	2.34
CLH-1-U	12.50	5.04	0.74	2.33	2.34
CLH-2-T	12.50	5.04	0.95	2.33	2.34
CLH-2-U	12.50	5.04	0.90	2.32	2.33
CLH-3-T	12.50	5.04	0.93	2.32	2.33
CLH-3-U	12.50	5.04	1.09	2.32	2.33

CLV: specimens prepared perpendicular to the bedding plane, CLH: specimens prepared parallel to the bedding plane.

The triaxial tests were performed in the geophysical imaging cell (GIC) at the Rock Fracture Dynamics Facility (RFDF) at the University of Toronto. The cell is equipped with ultrasonic-wave velocity stacks oriented along three orthogonal axes of X, Y and Z, enabling us to measure the evolution of compressional and shear wave velocities as a function of differential stresses. During the experiments, in addition to the axial deformational measuring unit of the Mechanical Testing Systems (MTS), two separate LVDTs close to the specimen outside the cell (integrated part of the GIC) were also used to measure axial deformation of the specimen. The diametral strain of the specimen was measured with an in-built cantilever system within the GIC.

The axial loading rate was controlled at a strain rate of 1.6×10^{-6}. The permeability of the specimens was measured with the pulse decay method (Brace et al. 1968). The servo-controlled load was kept on hold during the permeability measurement. A servo-control Quizix pump system (two pumps under independent constant control mode) was used to regulate the top and bottom pore pressures and to generate hydraulic pulses for permeability measurements under targeted axial stress levels up to the post failure region. Prior to the permeability measurement, the upstream and downstream storage factors of the testing cell were evaluated using a steel sample of same size as that of the rock specimens following methods outlined by Boulin et al. 2012.

3. Experimental results

Six tests were conducted on specimens parallel (3 samples) and perpendicular (3 samples) to the bedding plane under hydrostatic and differential stress conditions with a confining pressure of 5 MPa and an initial pore pressure of 3 MPa. The permeability of each specimen was measured at the initial hydrostatic and later differential stresses. Once a target differential stress was reached, a 1 MPa hydraulic pulse was applied to measure the permeability of the specimen. Figure 3-1 shows the representative stress-strain relationship of specimen CLH-1-U (cored parallel to the bedding plane) and the evolution of permeability with axial strain. Figure 3-2 shows the failure mode of specimen CLH-1-U and its 3D sketch corresponding to the seismic velocity measurement. Figure 3-3 shows the compressional wave velocities along three orthogonal axes and the permeability values measured at different axial stresses for specimen CLH-1-U. Figure 3-4 shows the representative stress-strain relationship of specimen CLV-3-T (cored perpendicular to the bedding plane) and the evolution of permeability with axial strain. Figure 3-5 shows the failure mode of specimen CLV-3-T and its 3D sketch corresponding to the seismic velocity measurement. Figure 3-6 shows the compressional wave velocities along three orthogonal axes and the permeability values measured at different axial stresses for specimen CLV-3-T.

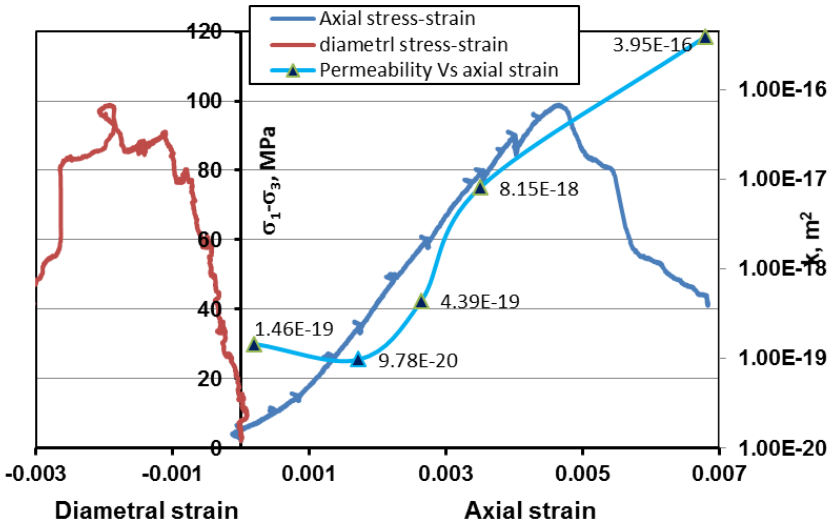

Figure 3-1. The stress-strain relationship of specimen CLH-1-U and the evolution of permeability with axial strain.

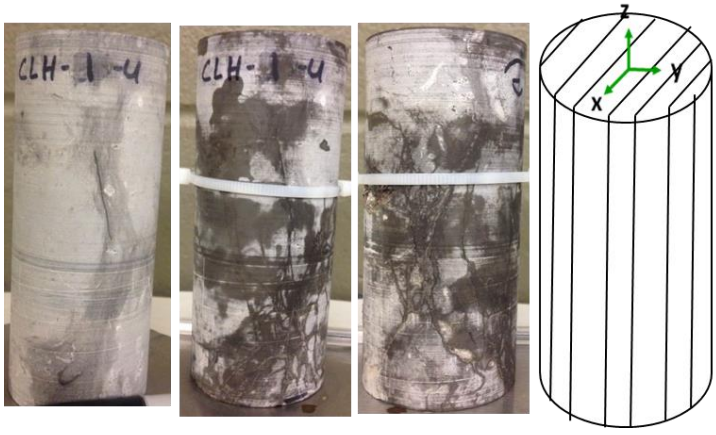

Figure 3-2. Failure mode of specimen CLH-1-U (left image shows intact specimen) and the 3D sketch corresponding to the seismic velocity measurement.

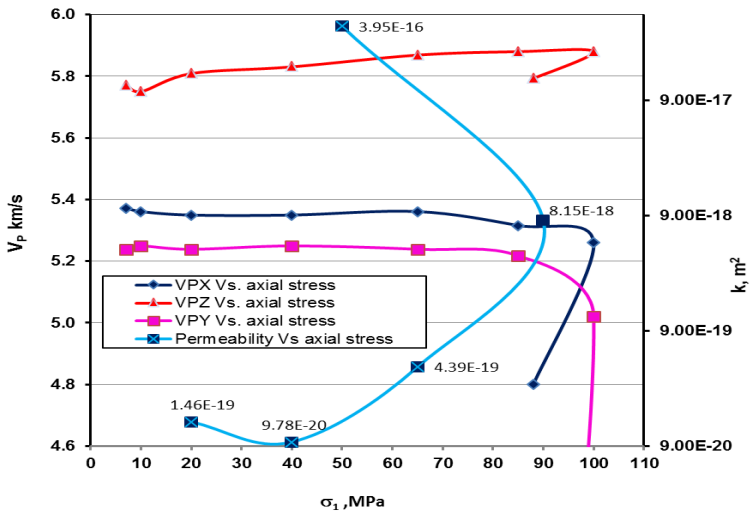

Figure 3-3. Compressional wave velocities along three orthogonal axes and the permeability values measured at different axial stresses for specimen CLH-1-U.

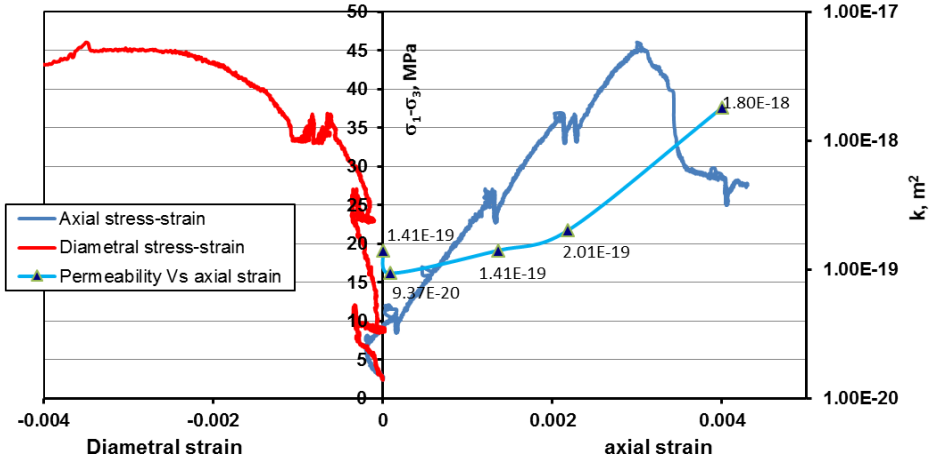

Figure 3-4. The stress-strain relationship of specimen CLV-3-T and the evolution of permeability with axial strain.

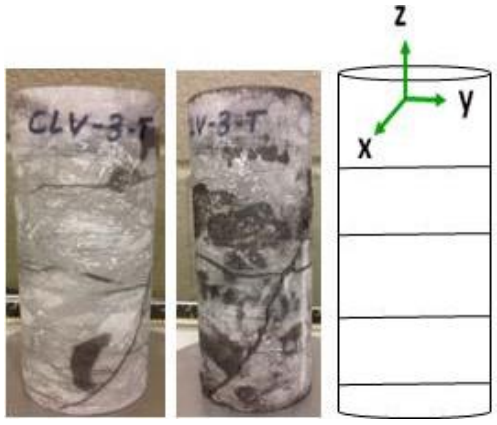

Figure 3-5. Failure mode of specimen CLV-3-T and the 3D sketch corresponding to the seismic velocity measurement.

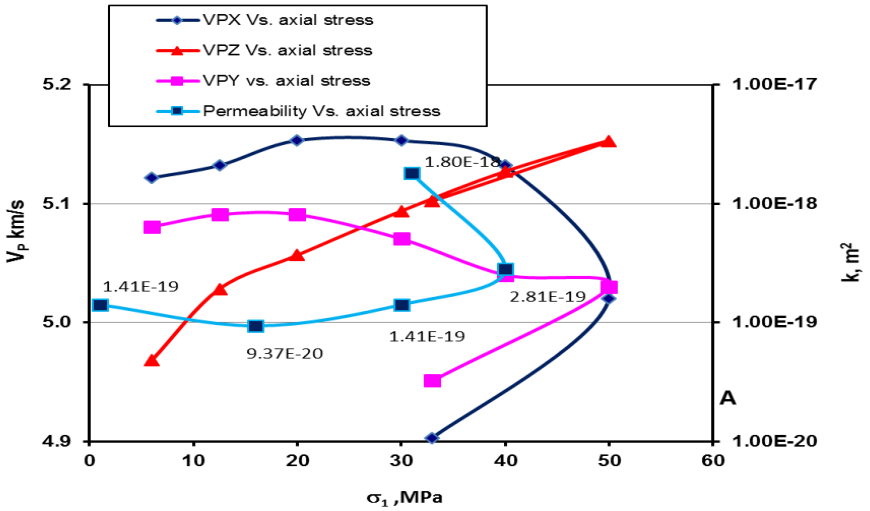

Figure 3-6. Compressional wave velocities along three orthogonal axes and the permeability values measured at different axial stresses for specimen CLV-3-T.

4. Numerical simulations of triaxial test results

The experimental results of triaxial tests were used for numerical investigation of the coupled hydro-mechanical behaviour of the Cobourg limestone. The constitutive relationship was developed to describe the stress-strain behaviour of the limestone. The constitutive relationship relates the stress increment to the strain increment

$$d\boldsymbol{\sigma} = \mathbf{D}(d\boldsymbol{\varepsilon} - d\boldsymbol{\varepsilon}^p)$$

where $d\boldsymbol{\sigma}$ is the increment of the stress tensor (written as a vector); $d\boldsymbol{\varepsilon}$ is the increment of total strain tensor (written as a vector); $d\boldsymbol{\varepsilon}^p$ is the increment of the plastic strain tensor (written as a vector); and $\mathbf{D}$ is the elastic stiffness tensor (written as a matrix).

The elastic stiffness tensor is transversely isotropic, with two principal directions, one parallel and one perpendicular to the bedding plane. Furthermore, the degradation of the Young's moduli with accumulated irreversible strain is taken into account.

The plastic strain, that is assumed to be a measure of damage, is obtained using a Mohr-Coulomb criterion, where the cohesion c and the friction angle ϕ are made directionally-dependent using the microstructure tensor approach (Pietruszczak and Mroz 2001). Strain hardening and post failure softening are taken into account by making those parameters vary with the effective plastic strain. Figure 4-1 shows the modelled stress-strain curves for the Cobourg limestone at two loading orientations for specimens CLV-3-T (perpendicular to the bedding plane) and CLH-1-U (parallel to the bedding plane). In order to understand the effect of the mechanical damage on the evolution of permeability, the computed plastic strain (x-axis) is plotted against the measured permeability (y-axis) under the defined loading conditions. Figure 4-2 shows the evolution of permeability with the computed plastic strain for both specimens CLH-1-U (β=90°) and CLV-3-T (β=0°), where β is the angle between the bedding plane and the horizontal axis X.

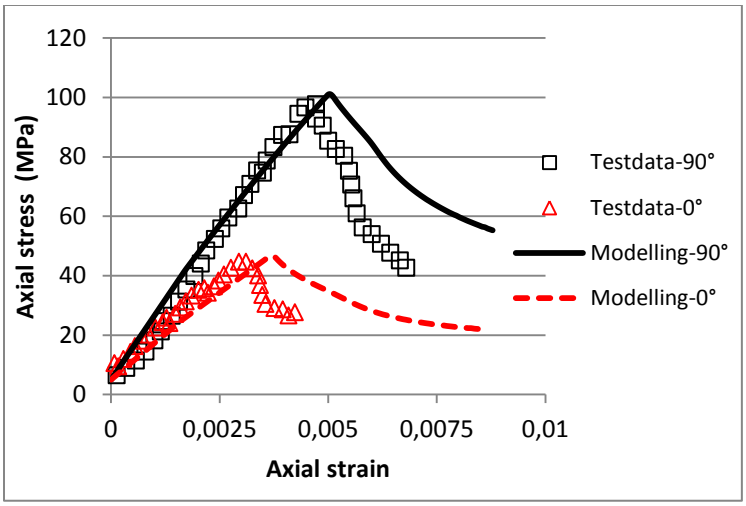

Figure 4-1. Experimental and modelling results on stress-strain relationship for specimens CLH-1-U (β=90°) and CLV-3-T (β=0°).

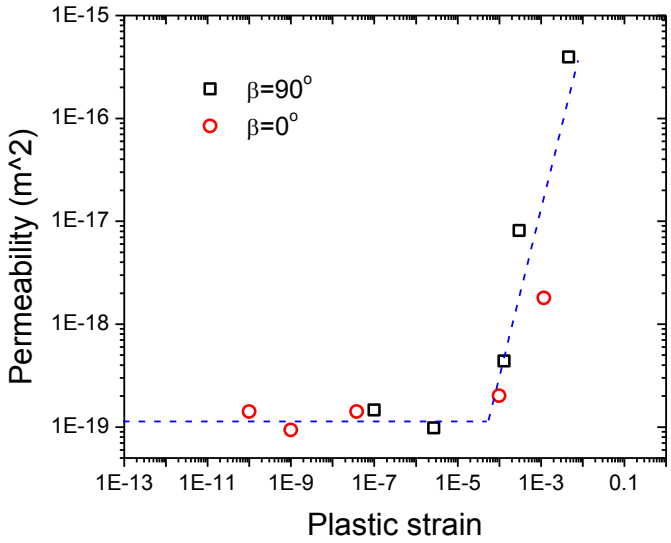

Figure 4-2. Evolution of permeability with the computed plastic strain for specimens CLH-1-U (β=90°) and CLV-3-T (β=0°).

5. Conclusion

The Cobourg limestone is an anisotropic material, and its strength and deformation behaviour are direction dependent. However, the permeability of the intact limestone does not show significant difference for rock specimens cored at two different orientations (i.e. parallel and perpendicular to the bedding plane). These permeability values measured with the transient method (i.e. pulse decay method) are comparable to the results measured with the conventional method (Selvadurai and Jenner 2012). The permeability measured post-failure is 2~3 orders of magnitude higher than that of intact rock. This means that the permeability of the highly damaged limestone due to excavation could be at least 3 orders of magnitude higher than that of the undamaged rock. The enhanced permeability of the

damaged rock must be considered in the safety assessment of the repository, and should be mitigated with sealing systems if needed. Using data from the experiment, a microstructure tensor-based, anisotropic, elastoplastic hardening-softening model was developed for the Cobourg limestone. The model is able to reproduce the inherent anisotropy due to bedding and the evolution of permeability with damage for both specimens CLH-1-U and CLV-3-T.

References

Boulin, P. F., Bretonnier, P., Glan, N., and Lombard, J. M. 2012. Contribution of the steady state method to water permeability measurement in very low permeability porous media, Oil and Gas Science and Technology-Rev. IFP Energies nouvelles, Doi: 0.2516/ogst/2011169.

Brace, W. F., Walsh, J. B., and Frangos, W.T. 1968. Permeability of granite under high pressure. J Geophys Res, 73(6): 2225–2236.

ISRM 1981a, Part 1: Suggested method for determining water content, porosity, density, absorption and related properties. ISRM Suggested Methods: Rock Characterization testing and monitoring. Int. Soc. Rock Mech. 81-89.

NWMO 2011. Geosynthesis. *OPG's deep geologic repository for low and intermediate level waste*. NWMO DGR-TR-2011-11.

Pietruszczak, S. and Mroz, Z. 2001. On failure criteria for anisotropic cohesive-frictional materials. *International Journal for Numerical and Analytical Methods in Geomechanics*, **25**, 509-524.

Selvadurai, A. P. S. and Jenner, L. 2012. Radial flow permeability testing of an argillaceous limestone. Ground Water, Doi:10.111/j1745-6584.2012.00932.x.